Journal of Surface Analysis Vol.14, No. 4 (2008) pp. 305-311
Martin P Seah Sputtering, Cluster Primary Ions and Static SIMS

Invited Paper

Sputtering, Cluster Primary Ions and Static SIMS

Martin P Seah*
Quality of Life Division, National Physical Laboratory, Teddington, Middlesex TW11 0LW, UK
**martin.seah@npl.co.uk*

(Received: November 26, 2007; Accepted: January 18, 2008)

Sputtering using cluster primary ion beams is very important for the future development of static SIMS and the SIMS depth profiling of organic layers. However, different results from different laboratories may be confusing. Analytical models have an important function for enabling the prediction of behaviour for practical analysis. Sigmund's model for sputtering, often used in surface analysis, is helpful and accurate in the linear cascade regime. However, for cluster sputtering this is no longer the case and spike effects need evaluation. Evidence will be presented of the spike model validity for clusters of up to more than 10 atoms over 3 orders of magnitude in sputtering yield. Using data from one primary ion, extremely good descriptions of measurements reported with other primary ions can then be achieved.

This theory is then used to evaluate the molecular ion yield behaviour of interest in the static SIMS of organics. This leads to universal dependencies for the de-protonated molecular ion yields, relating all primary ions, both single atom and cluster, which are illustrated by experimental data over 5 decades of emission intensity. This formulation permits the prediction of the $(M-H)^-$ secondary ion yield for different, or new, primary ion sources. It is shown how further gains are predicted. For analysing materials, raising the molecular secondary ion yield is extremely helpful but it is the ratio of this yield to the disappearance cross-section (the efficiency) that is critical. The relation of the damage and disappearance cross sections is formulated. Data are evaluated and a description is given to show how these cross sections are related and to provide a further universal relation for the efficiency/yield dependence of all cluster ions.

1. Introduction

Static secondary ion mass spectrometry (SIMS) has emerged in recent years as a powerful tool for studying organic materials at surfaces. Since the turn of the century, a new range of instruments has become available with sufficient control that data are now reproducible from laboratory to laboratory [1] with the level of confidence [2] previously only available in Auger and X-ray photoelectron spectroscopies and the dynamic SIMS of semiconductor materials. This improvement in static SIMS opens the gateway to studies of a wide new range of organic and biological materials and to extend that activity from the current few expert laboratories more widely.

It is generally accepted that there is a degree of speciation available in static SIMS, that is not available in AES or XPS, to analyse and unravel the structure of complex molecules at surfaces. Recent developments in gentle-SIMS (G-SIMS) [3,4] allow the main molecular fragments to be identified and G-SIMS with fragmentation pathway mapping (G-SIMS FPM) [5,6] allows the reconstruction of the molecule from the static SIMS data. Combined with Simplified Molecular Input Line Entry Specification (SMILES) [7] analysis, these procedures allow a completely new degree of interpretation to be realised.

In addition to these developments, there has been a plethora of new primary ion sources that lead to apparently different spectra with different proposed advantages [8,9]. For static SIMS, studies include primary ions of Ar^+, Xe^+, Ga^+, Cs^+, SF_5^+, Au^+, Au_2^+, Au_3^+, In^+, Bi^+ and so on. In the present paper, the differences between these ion sources are discussed in order to provide a unifying overview. To do this, we start with the background to sputtering, sputtering with cluster ions and finally the static SIMS of one particular organic

molecule, Irganox 1010.

2. Sputtering

The most powerful of the sputtering theories is that of Sigmund [10] called the linear cascade model. This theory leads to a ready presentation of sputtering yields using commonly available input data. Matsunami *et al.* [11] and many others have looked at semi-empirical descriptions of the input functions and have added threshold and correction factors. Seah *et al.* [12,13], more recently, have re-analysed Matsunami *et al.*'s [11] description and found that a significant improvement is achieved by replacing their overall scaling constant Q by a term dependent on the atomic density, as discussed in Sigmund's earlier work [10]. Using this development, Seah *et al*. provide semi-empirical equations that fit all yields studied for Ne^+, Ar^+ and Xe^+ sputtering to a standard deviation of 12%. The figure of 12% is probably limited by the data repeatability. This showed that the linear cascade model was an excellent description of sputtering.

For sputtering with cluster sources, the deposited energy density is much higher and Sigmund and Claussen [14] proposed that the thermal spike following the bombarding primary ion would then lead to thermal evaporation in addition to the linear cascade sputtering. This thermal spike led to the emission of lower energy ions than the linear cascade and followed the latter, temporally, in the ensuing picoseconds.

The sputtering yield according to Sigmund and Claussen's model may be written [15]:

$$Y = Y_{\text{lin}} + Y_{\text{th}} \qquad (1)$$

where,

$$Y = Y_{\text{lin}}\left[1 + B\,g\left(U_{\text{o}}/kT\right)Y_{\text{lin}}\right] \qquad (2)$$

B is a constant for the sample and $g(U_o/kT)$ is a function rising from 0 at $T = 0$ to 1 at very high T. Here T is the initial core temperature of the spike and depends on the rate of energy deposition of the primary ion at the surface.

Seah showed that this model described the energy, E, dependence and the effect of cluster size, n, for the sputtering of many systems by cluster ions. Figure 1(a) [16] shows the validity of the model for the data for sputtering gold by Au_n^+ for $1 \le n \le 13$. The fit is remarkably good. Figure 1(b) shows the individual contributions of Y_{lin} and Y in these calculations. For $Y \le 10$, the Y_{th} part is very small. However, as the yield rises, the thermal spike contribution increases until, eventually, it is some 50 times greater than the linear part. In an analysis of published sputtering yields of Au by Ne^+, Ar^+, Xe^+ and Xe_2^+, using parameters derived from the study in Fig. 1, Seah was then able to predict the absolute yields and smooth transition from the linear cascade to the regime where Y_{th} dominates, with great accuracy, as shown in Fig. 2. This supports both of Sigmund's theories.

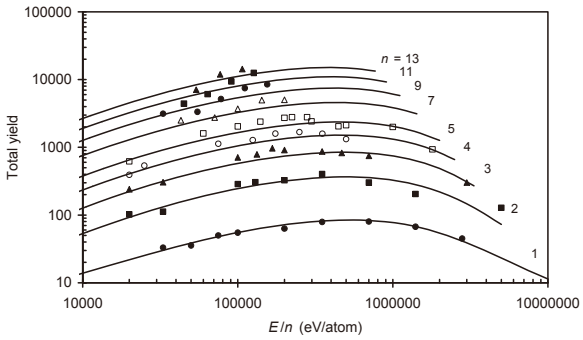

(a)

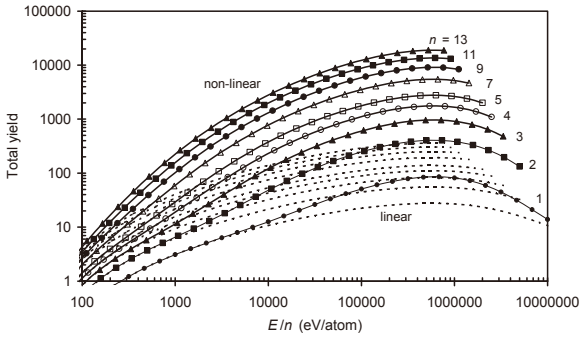

(b)

Figure 1. (a) The total sputtering yield data for Au sputtered by Au_n^+ of Bouneau *et al*. [16], together with the predictions of Eq. (2) for the following n values: 1 (●), 2 (■), 3 (▲), 4 (○), 5 (□), 7 (Δ), 9 (●), 11 (■) and 13 (▲). (b) The energy dependence of Y (—) and Y_{lin} (---) for Au sputtered by Au_n^+, after Seah [15].

These predictions provided a background theory to consider the more difficult issue of the static SIMS of organics.

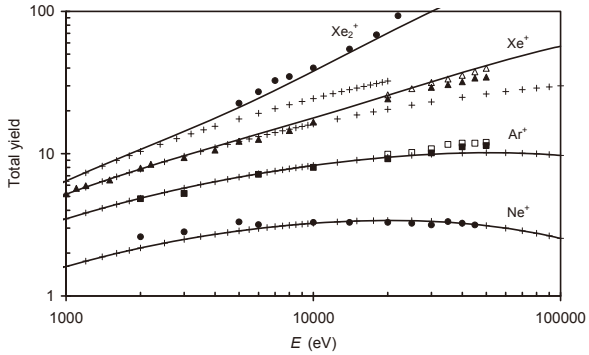

Figure 2. The experimental data of Olivia-Florio *et al*. [17], (filled symbols), and Nenadović *et al*. [18], (empty symbols) for the sputtering of Au by Ne^+ (●), Ar^+ (■,□), Xe^+ (▲,Δ) and Xe_2^+ (●). The calculations show Y_{lin} (+), which should not correlate with the data, and Y (—), which should correlate with the data, after Seah [15].

3. The Static SIMS of Irganox 1010

The best set of data to consider are those by Kersting *et al.* [19] and Kollmer [20], shown in Figure 3. These are for a spin cast layer, thought to be a monolayer of Irganox 1010 on low density polyethylene. The reader will note that there are some general trends but it is difficult to see why the data presented have the values shown or what would happen for completely new sources. To understand these trends, Seah used Sigmund and Claussen's theory [14] applied to a general organic sample to calculate the sputtering yield for Au, Au_2^+ and Au_3^+. This was then matched to Kersting *et al.* [19] and Kollmer's [20] data for the total ion yield, as shown in Fig. 4. It was expected that the total ion yield and the sputtering yield would be related and this plot confirms that view. Figure 5(a) shows the relation of the important de-protonated molecular ion yield, $Y(\text{M-H})^-$, as a function of the total ion yield for Au^+, Au_2^+ and Au_3^+. The squared relation shown is an excellent description. All the clusters simply overlap in behaviour and the enhancement of $Y(\text{M-H})^-$ over Y increases as the energy rises so that the effect for one ion cluster at low energy is the same as that of another at higher energy.

Figure 5(b) plots the results for all ions [15]. It is clear now that the chemical nature of these primary ions is relatively unimportant and that for all these ions:

$$Y(\text{M}-\text{H})^- \propto Y^2 \tag{3}$$

Equation (3) is the first such correlation in static SIMS. The power of 2 is not expected to be valid for the yields of significantly smaller molecules.

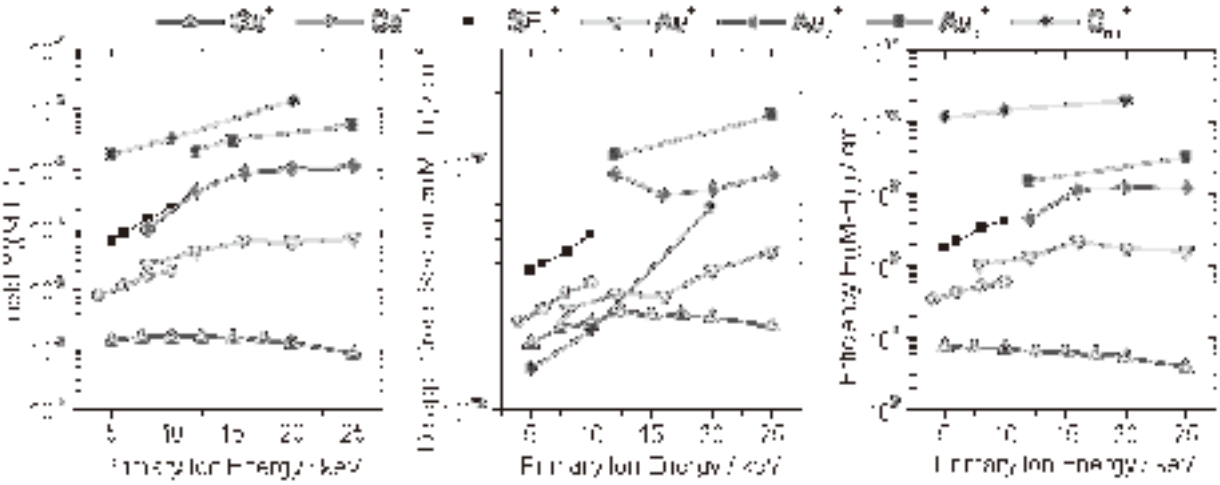

Figure 3. Data from Kersting *et al*. [19] and Kollmer [20] for $Y(\text{M-H})^-$, σ_{Dis} and the efficiency (courtesy R. Kersting). The primary ion type is shown by the symbols at the top of the Figure.

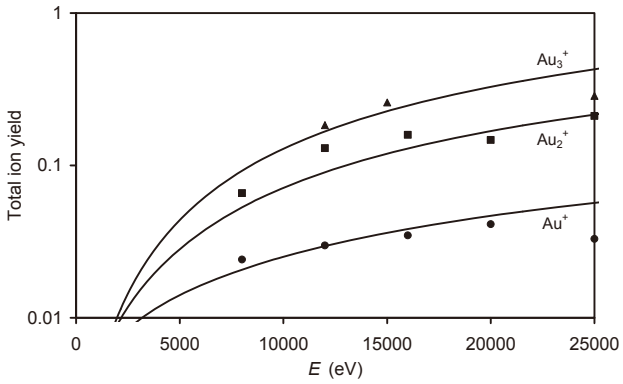

Figure 4. Comparison of the total ion yield with the calculated sputtering yield for Irganox 1010 using Au_n^+ primary ions at 45° incidence angle, after Seah [15].

If, instead of using the total ion yields, which are measured experimentally, we calculate the yield, Figure 5 could be turned into a predictive plot. For new sources, we can calculate a yield but cannot provide an experimental total ion yield. Using Sigmund and Claussen's theory for a typical organic substrate, it is found that [21]:

$$Y \propto \left(nY_{\text{lin}}\right)^2 \tag{4}$$

and, by eliminating sample-dependent parameters,

$$Y_{\text{lin}} \propto Z_1^{1.22} s_{\text{n}}(\varepsilon) \tag{5}$$

where Z_1 is the atomic number of one of the cluster atoms of the primary ion and $s_n(\varepsilon)$ is the universal function of the reduced energy ε that contributes to the nuclear stopping cross section. By plotting Y(M-H)$^-$ versus $(Y^*)^2$ where Y^* is $nZ_1^{1.22} s_{\text{n}}(\varepsilon)$, a diagram very similar to Figure 5 is obtained, supporting the view that the total ion yield does reflect Y and supporting Eq. (3). Figure 6 enlarges the upper portion of this plot. In Fig. 6 are the data points for Cs^+, SF_5^+, Au^+, Au_2^+, Au_3^+ and C_{60}^+ from experiment and, added predictions for Au_5^+, Au_7^+, Bi^+, Bi_2^+, Bi_5^+, Bi_7^+ and C_{70}^+. The predictions use Eq. (5) with the proportionality constant given by the experimental data.

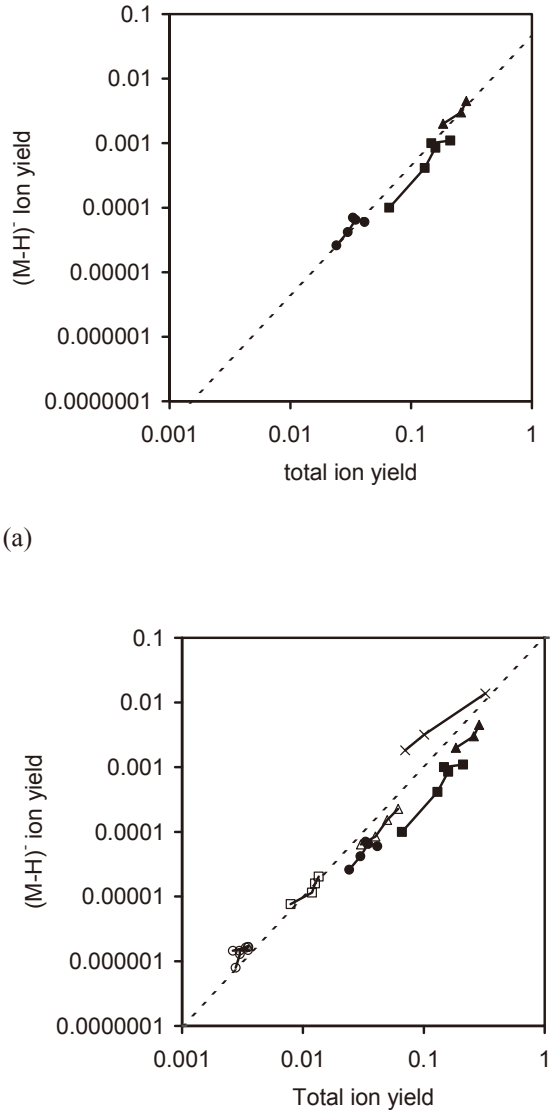

Figure 5. (a) Correlation of the (M-H)$^-$ secondary ion yield data for Irganox 1010 on low density polyethylene at 45° incidence angle from Kersting *et al*. [17] with the total ion yield, (●) Au^+, (■) Au_2^+, (▲) Au_3^+. and, b) the correlation for all primary ions, (○) Ga^+, (□) Cs^+, (Δ) SF_5^+, (●) Au^+, (■) Au_2^+, (▲) Au_3^+, (×) C_{60}^+, after Seah [15].

Figure 6 is the first prediction of de-protonated ion yields and was presented at the 44th IUVSTA Workshop on Sputtering and Ion Emission by Cluster Beams in April 2007. Kersting and Kollmer noted that they had new data confirming that the Bi_n^+ predictions were valid.

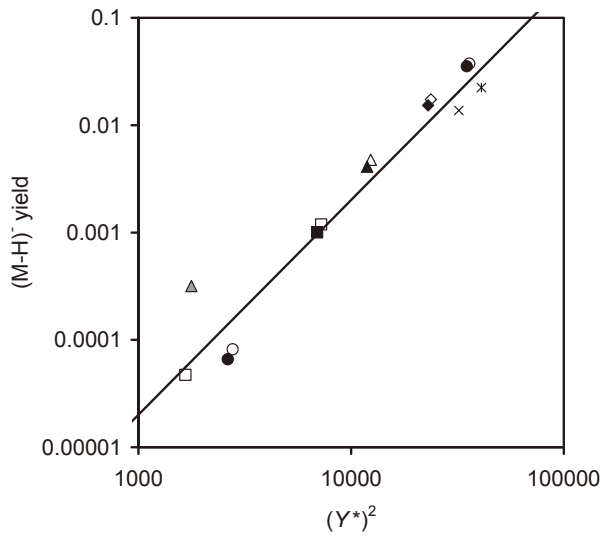

Figure 6. Predictions for Au_5^+, Au_7^+, C_{70}^+, Bi_1^+, Bi_2^+, Bi_3^+ and Bi_5^+ based on Eq. (5), (□) Cs^+Δ( ) SF_5^+, (●) Au^+, (■) Au_2^+, (▲) Au_3^+, (♦) Au_5^+, (●) Au_7^+, (×) C_{60}^+, (○) Bi^+, (□) Bi_2^+, (Δ) Bi_3^+, (◊) Bi_5^+, (○) Bi_7^+, (∗) C_{70}^+. The Au_7^+ and Bi_7^+ have similar symbols to Au^+ and Bi^+ but have ordinate values 3 orders higher. The line shows a dependence on $(Y^*)^4$, after Seah [19].

4. Damage Effects in Static SIMS

Predicting the cluster sources to give high values of $Y(\text{M-H})^-$ is important but the central plot in Fig. 3 shows that the damage changes and that one needs a prediction for the disappearance cross section, σ_{Dis}, to check that increasing the yield does not lead to a poorer signal per molecule present. The figure of merit often used here is the efficiency, shown to the right in Fig. 3, where

$$\text{efficiency} = Y(\text{M}-\text{H})^- / \sigma_{\text{Dis}} \qquad (6)$$

From the data in Fig. 3 and other data in Kersting *et al.* [19] and Kollmer's [20] work, giving the total ion yield, the plot of σ_{Dis} versus total ion yield shown in Fig. 7 may be generated.

The disappearance cross section arises from two main effects; damage to the sample by the primary ion beam with cross section σ_{D} and sputter removal of the surface molecules with molecular area A_{m}. Thus, approximately [21]

$$\sigma_{\text{Dis}} = \sigma_{\text{D}} + YA_{\text{m}} \qquad (7)$$

where

$$\sigma_{\text{D}} = \pi\left(r_{\text{i}} + r_m\right)^2 \qquad (8)$$

r_1 being the radius of the damaged region from the primary ion beam and $\pi r_{\text{m}}^2 = A_{\text{m}}$. From our knowledge of those systems, reasonable values for r_1, r_{m} and A_{m} are 1.9 nm, 1.25 nm and 4.9 nm^2, respectively. The curve for Eq. (7) is shown in Figure 7 with Y related to the total ion yield from the data of Shard *et al.* [22] where a yield of 97 molecules related to a total ion yield of 0.3.

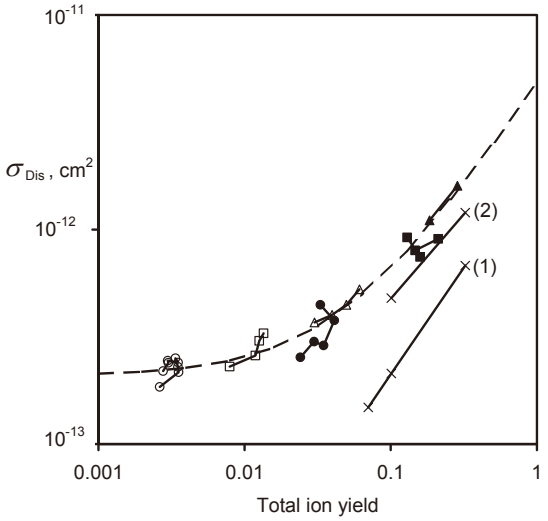

Figure 7. Correlation of the measured σ_{Dis} and the total ion yield from Kersting *et al.* and Kollmer, (○) Ga^+, (□) Cs^+, (Δ) SF_5^+, (●) Au^+, (■) Au_2^+, (▲) Au_3^+ and (×) C_{60}^+. The dashed line shows a correlation with the total ion yield as in Eq. (7), "(1)" original C_{60}^+ data[19,20], "(2)" revised C_{60}^+ data, after Seah [19].

The C_{60}^+ data shown with the "(1)" are well away from the curve and it was reasoned that C_{60}^+, unlike the other ions, would remove a first layer and expose a second layer if the sample had more than one monolayer on the surface. In this case, it was estimated that the C_{60}^+ data were for a film that was too thick. At the 44th IUVSTA meeting, Kersting and Kollmer agreed and said that the solution used to deposit the layer had thickened since recording the other data and had deposited too thick a layer. New data provided by Kersting and Kollmer showed higher σ_{Dis} values which are plotted with the "(2)" in much better agreement with the curve.

These results allow Fig. 8 to be plotted for the efficiency. This shows excellent consistency of data from different primary ion species. For low yields, the efficiency is proportional to $Y(\text{M-H})^-$ and, at high yields, from Eqs (3) and (7), proportional to the square root of $Y(\text{M-H})^-$. Thus, the efficiency continues to rise with the yield, albeit at a slower rate.

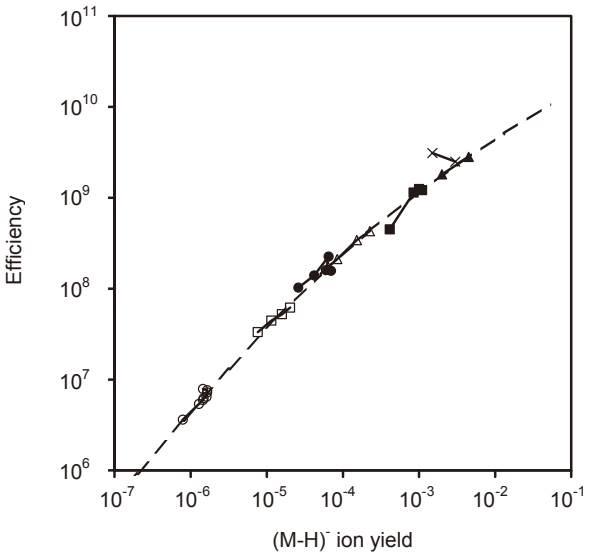

Figure 8. Correlation from Fig. 7, (○) Ga^+, (□) Cs^+, (Δ) SF_5^+, (●) Au^+, (■) Au_2^+, (▲) Au_3^+, (×) updated for the more recent C_{60}^+ data of Kersting and Kollmer. The dashed line shows the correlation with σ_{Dis} from Eq. (7), after Seah [19].

The data in Fig. 8 were recorded on different instruments in different laboratories at different times by different researchers. The consistency shows what can be achieved if procedures are carefully documented and properly followed.

5. Conclusions

In this brief review we have demonstrated the validity of the linear cascade approach for calculating sputtering yields for monatomic primary ions. For cluster primary ions, the extension of the thermal spike model provides an excellent description. This leads to the important relation

$$Y \propto \left(nY_{\text{lin}}\right)^2 \tag{9}$$

which may be applied to organic systems. Figures 5 and 8 show that the cluster ion effects in SIMS are governed mainly by physical, and not chemical, attributes. The results of Figs. 5 and 6 show the important relation of Eq. (3). Figure 5 allows the behaviour of new cluster primary ion sources to be predicted. Figures 7 and 8 show that σ_{Dis} and the efficiency both rise monatonically with Y and $Y(\text{M-H})^-$, respectively, in a smooth and simple manner.

The systematising of the original data, the objective of the study, has been achieved, demonstrating a range of new relationships. These effects are all simple in concept but allow the relative merits of different existing and future primary ion sources to be understood. These effects can generate significant non-linearities in measurements that need to be included, in particular, in interpreting SIMS depth profile data for organics.

6. Acknowledgements

The author would like to thank I S Gilmore, F M Green and A G Shard for helpful comments and both F Kollmer and R Kersting for Fig. 3 and for helpful information and unpublished data for Bi_n^+ and C_{60}^+ ions. This work is supported by the National Measurement System of the UK Department for Innovation, Universities and Skills through the Chemical and Biological Metrology Programme. The author would also like to thank the organisers of PSA-07 for inviting this review.

7. References

[1] I. S. Gilmore, M. P. Seah and F. M. Green, Surf. Interface Anal., 37, 651 (2005).
[2] I. S. Gilmore, F. M. Green and M. P. Seah, Surf. Interface Anal., 39, 817 (2007).
[3] I. S. Gilmore and M. P. Seah, Appl. Surf. Sci., 161, 465 (2000).
[4] I. S. Gilmore and M. P. Seah, Appl. Surf. Sci., 203-204, 551 (2003).
[5] I. S. Gilmore and M. P. Seah, Appl. Surf. Sci., 231-232, 224 (2004).
[6] I. S. Gilmore, F. M. Green, and M. P. Seah, Appl. Surf. Sci., 252, 6601 (2006).
[7] F. M. Green, I. S. Gilmore and M. P. Seah, Proc SIMS XVI, Appl. Surf. Sci. in the press, published on line 9 May 2008 doi : 10. 1016 / j. apsusc. 2008. 05. 087.
[8] A. Wucher, Appl. Surf. Sci., 252, 6482 (2006).
[9] B. J. Garrison, Appl. Surf. Sci., 252, 6409 (2006).
[10] P. Sigmund, Phys. Rev. 184, 383 (1969).
[11] N. Matsunami, Y. Yamamura, Y. Hikawa, N. Itoh, Y. Kazumata, S. Miyagaura, K. Morita, R. Shimizu and H. Tawara, Atomic Data and Nucl. Data Tables, 31, 1 (1984).
[12] M. P. Seah, C. A. Clifford, F. M. Green and I. S. Gilmore, Surf. Interface Anal., 37, 444 (2005).
[13] M. P. Seah, Nucl. Ins. Meths. B., 229, 348 (2005).

[14] P. Sigmund and C. Claussen, J. Appl. Phys. 52, 990 (1981).
[15] M. P. Seah, Surf. Interface Anal. 39, 634 (2007).
[16] S. Bouneau, A. Brunelle, S. Della-Negra, J. P. Depauw, D. Jacquet, Y. Le Beyec, M. Pautrat, M. Fallavier, J. C. Poizat and H. H. Andersen, Phys. Rev. B, 65, 144106 (2002).
[17] A. Olivia-Florio, R. A. Baragiola, M. M. Jakas, E. V. Alonso and J. Ferron, Phys. Rev. B. 35, 2198 (1987).
[18] T. M. Nenadović, Z. B. Fotirić and T. S. Dimitrijević, Surf. Sci. 33, 607 (1972).
[19] R. Kersting, B. Hagenhoff, F. Kollmer, R. Möllers and E. Niehuis, Appl. Surf. Sci., 231-232, 261 (2004).
[20] F. Kollmer, Appl. Surf. Sci., 231-232, 153 (2004).
[21] M. P. Seah, Surf. Interface Anal, 39, 890 (2007)
[22] A. G. Shard, P. Brewer, F. M. Green and I. S. Gilmore, Surf. Interface Anal., 39, 294 (2007).

Discussion between referees and authors

Referee 1:

The paper successfully reports the evaluation of the spike model for the sputtering using cluster primary ion beam with extended evaluation of the molecular ion yield behavior and other important parameters such as damage and disappearance cross sections and so on. The referee regards the paper is in a high quality and deserves for publication without any changes or corrections.

[Author]

Many thanks for your kind and positive comments.

Referee 2:

Full spell should be given to the first use of abbreviation, e.g. G-SIMS, SMILES.

[Author]

Yes, this should have been done and is now done.